Parametric study of ductile moment-resisting steel frames. First step for Eurocode 8 calibration.

L. Sanchez-Ricart[1,*] and A. Plumier[2]

[1]*Departamento de Estructuras y Construcción, Universidad de Cartagena, Campus Alfonso XIII - 30203 Cartagena, Murcia, España.*

[2]*Département ARGENCO, Université de Liège, Chemin des Chevreuils 1, (Bât. B52) Sart Tilman - 4000 Liège, Belgique.*

SUMMARY

A parametric study of 13,608 ductile Moment-Resisting Steel Frames (MRSF) designed according to Eurocode 3 and Eurocode 8 is performed. A flowchart for the evaluation of the seismic-resistant capacity of the designed frames is developed based on the N2 method. The design structural overstrength, the ductility supply, the plastic redistribution parameter, the supply reduction factor and the performance ratio of the frames under study are analysed. The 13,608 designed frames under study have performance ratios higher than one mostly due to the high values of design structural overstrength, showing that the seismic supply produced by Eurocode 3 and Eurocode 8 restrains are always higher than the seismic demand.

KEY WORDS: reduction factor; steel frames; seismic performance; global ductility; structural overstrength; code calibration

1. INTRODUCTION

The conceptual design is a basic step when designing a structural system [1]. Once the conceptual design has been decided, the level of freedom in the design process is limited and the performance of the structure is almost defined. A-priori estimations of global structural parameters are useful to determine the most convenient conceptual design in displacement-based or force-based design [2].
The study presented here is a first step in a work with two main long-term objectives:
1. To improve the elastic design procedures of Eurocode 8 [3] for MRSF.
2. To provide guidance for conceptual design based on a-priori estimation of global structural parameters.
A calibration flux diagram based on the N2 method [4] is developed. It benefits from the background knowledge in the response of Single-Degree-of-Freedom (SDOF) systems. In the N2 method, the structural damage is computed using the spectral intensity prescribed in the code. In the present study, the intensity that the structural system is able to sustain will be estimated. The results obtained are based on the assumptions of the N2 method.

To the authors' knowledge, the available information to support decisions on the design reduction factor in seismic codes shows significant dispersion in the evaluated values. If the dispersion is real, large samples will be necessary in order to obtain representative results. Besides, the structures under study must be designed according to the structural codes if realistic values of structural overstrength and ductility supply are to be assessed.

* Correspondance to: L.Sanchez-Ricart, Universidad de Cartagena, Departamento Estructuras y Construcción, Campus Alfonso XIII, Despacho 118, Paseo Alfonso XIII, 52, 30203, Cartagena, Murcia, Spain. Email: luis.sricart@upct.es Telephone: +34 968 32 57 41 Mobile: +34 656 877 401

With this aim in mind, a group of structural engineers could be chosen to solve some benchmark problems or evaluate the capacity of existing buildings. These approaches would be time consuming and would not provide representative results.

Instead, we solve the problem by reversing what is normal practice in structural design. We choose a structural type and configuration irrespective of the initial constraints of the project. This puts us in a situation in which normal structural engineering practices are not tested but the structural codes themselves are tested. This approach allows for performing the work routinely and provides large samples that will allow us to analyse the nature of the dispersion. The design and evaluation of MRSF according to Eurocode 3 [5] and Eurocode 8 has been implemented in a computer program, which will serve for the calibration of Eurocode 8.

The choice of the present approach is not without drawbacks. The most convenient structural type must be selected in the conceptual design. Good selection of the structural type will reduce the values of the design structural overstrength. In this study, the conceptual design is nonexistent and, therefore, can only be understood as a test of Eurocode 3 and Eurocode 8 in themselves, in a wide range of situations for a given structural type, code interpretation and conceptual design.

In the future, when other structural types will be studied, the database generated by the program will also serve to provide guidance for conceptual design. Low values of the design structural overstrength will inform designers of the convenience of the structural type for each particular situation.

2. COMPONENTS OF THE REDUCTION FACTOR AND PERFORMANCE RATIO

Figure 1 shows the elastic behaviour and the pushover analysis of a structural system that has been designed to fulfil all the requirements of the structural codes under gravity and seismic loads. The two dashed lines represent constant values of Peak Ground Acceleration (PGA). a_d is the value of PGA used to design the structural system, and a_u is the maximum value of PGA for which the designed structural system is able to guarantee life safety. The design PGA, a_d, is to demand or requirement what the ultimate PGA, a_u, is to supply or capacity.

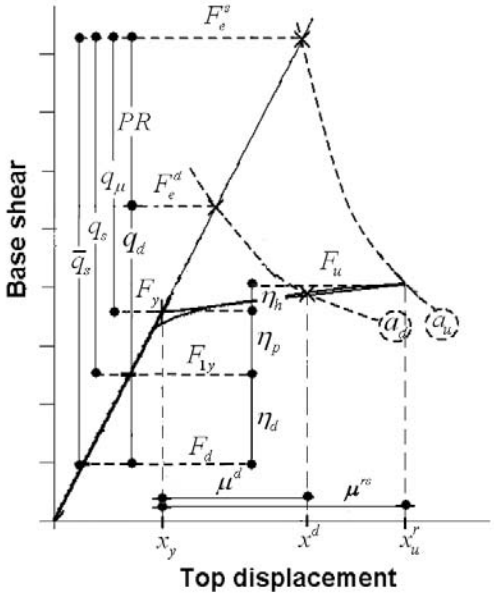

Figure 1. Pushover analysis of an eight-storey MRSF designed according to Eurocode 3 and Eurocode 8.

F_e^d and F_e^s are the base shears induced in the equivalent elastic structural system by the elastic spectrum of the seismic code for a value of PGA equal to a_d and a_u, respectively.

The elastic spectum is reduced to the design spectrum in seismic codes. It is assumed that if the structural system is designed to resist elastically the design spectrum, it will be able to resist the spectral intensity of the elastic spectrum thanks to the capacity of the structural system beyond the elastic limit. The design base shear, F_d, is the base shear induced by the design spectrum for a value

of PGA equal to a_d.

F_{1y} is the base shear at first yield (formation of first plastic hinge). F_{1v} is to seismic capacity what F_d is to seismic demand or requirement. Beyond the elastic limit, F_y is the base shear when the structure yields at the global level and F_u is the base shear related with the ultimate capacity of the structure.

A first component of the structural overstrength that we will name "design structural overstrength" is defined in order to account for the ratio of supply to demand in the linear range at the global structural level:

$$\eta_d = \frac{F_{1y}}{F_d} \tag{1}$$

Values of η_d greater than one are not intended in the structural design, since they are representative of resistance exceeding the performance objective of the Ultimate Limit State (ULS). However, η_d will frequently be much higher than one. Among others, sources of η_d are:

1. Member proportioning due to Serviceability Limit State (SLS) and ULS requirements under gravity loads.
2. Application of capacity design criteria.
3. Fulfilment of the SLS requirements under seismic loads.
4. Dimensions of the structural elements chosen from a discrete collection.
5. Over-design preferred to time consuming optimisation.

Once the base shear that produces the first yield is reached, the ductility of the materials and the yielding of the members allow the redistribution of internal forces. A second source of structural overstrength is defined, where the subscript "p" denotes "**p**lastic redistribution":

$$\eta_p = \frac{F_y}{F_{1y}} \tag{2}$$

Once the structure yields at the global level, the base shear can increase due to the strain hardening or if the plastic mechanism is not fully developed. A third component of structural overstrength is defined, in which the subscript "h" denotes "structural **h**ardening":

$$\eta_h = \frac{F_u}{F_y} \tag{3}$$

The total structural overstrength, η, will be the product of the three previous components:

$$\eta = \eta_d \cdot \eta_p \cdot \eta_h \tag{4}$$

The "reduced global ductility supply", μ^{rs}, is defined as the ratio of the reduced ultimate top displacement, x_u^r, to the top displacement at the structural yield of the equivalent bilinear diagram, x_y, where the adjective "reduced" applies because the influence of cyclic damage is implicitly included in the estimation of the ultimate capacity:

$$\mu^{rs} = \frac{x_u^r}{x_y} \tag{5}$$

Many formulations have been proposed in the literature relating to SDOF systems to account for the resistance-capacity provided by the ductility supply with an artificial reduction in the elastic response spectrum (see for example references [6-9]). In order to benefit from the background on the seismic response of bilinear SDOF systems, the increase in the system capacity to resist a seismic event, mainly due to hysteretic energy dissipation capacity and due to the increase in the effective periods, will be accounted for with the "ductility reduction factor", q_μ:

$$q_\mu = \frac{F_e^s}{F_y} \tag{6}$$

The "performance ratio", PR, is the ratio of the equivalent base shear supply to the equivalent base shear demand in the elastic structural system:

$$PR = \frac{F_e^s}{F_e^d} \tag{7}$$

The dashed line with constant value a_d cuts the pushover curve at "the top displacement demand", x^d (see Figure 1). The top displacement demand divided by the yield displacement is the "global ductility demand", μ^d:

$$\mu^d = \frac{x^d}{x_y} \tag{8}$$

The seismic code allows a reduction from the elastic spectrum to the design one. The aim is to account for the structural capacity in the non-linear range with an artificial reduction in the seismic action. The "design reduction factor", q_d, is defined as the effective reduction of the base shear forces in the seismic code:

$$q_d = \frac{F_e^d}{F_d} \tag{9}$$

F_d is to demand what F_{1y} is to supply. F_e^d is to demand what F_e^s is to supply. From this analogy, a first definition of "supply reduction factor" is obvious if the supply base shears replace the demand base shears in equation (9):

$$q_s = \frac{F_e^s}{F_{1y}} \tag{10}$$

If the right hand side of equation (10) is multiplied and divided by F_y, the supply reduction factor can be rewritten as the product of the overstrength due to plastic redistribution of internal forces times the ductility reduction factor. This is, for example, the approach of the ECCS Manual on Design of Steel Structures in Seismic Zones (see reference [10]):

$$q_s = \eta_p \cdot q_\mu \tag{11}$$

The idea that the "design structural overstrength", η_d, can be accounted for when evaluating the "supply reduction factor" is widely accepted in the technical literature. For example, in ATC-19 "Structural Response Modification Factors" [11], the method proposed for a systematic determination of reduction factor (R) includes the design structural overstrength. If this is the case, a second definition of supply reduction factor, $\overline{q}_s$, would be possible:

$$\overline{q}_s = \eta_d \cdot q_s \tag{12}$$

Knowledge in earthquake engineering has been largely enhanced due to post-earthquake investigations. Structural performances observed after past earthquakes have been used to support decisions adopted in seismic codes. Since the development of seismic codes is partially based on observed structural performance under real earthquakes, variables related to the "actual" structural behaviour are required. The adjective "actual" will thus imply "real" and "unknown". Laboratory tests of full-scale structures indicate values of actual resistance that are very important when compared with the assumed resistance. The superscript "a" denotes "actual", and it recalls that the "actual" behaviour of the building can differ largely from the behaviour assumed by the code. a_u^a is the actual ultimate PGA. a_u^a is the maximum value of PGA for which the actual structural system is able to guarantee life safety. F_e^{as} is the maximum base shear in the elastic system for a value of PGA equal to a_u^a. In order to account for the ratio of the actual to the assumed capacity to resist an earthquake, a fourth component of structural overstrength is defined:

$$\eta_a = \frac{F_e^{as}}{F_e^s} \tag{13}$$

Calibration of the design spectrum of the seismic code from the performance of the buildings under past earthquakes is frequent (see references [11-13]). This approach implicitly includes not only η_d, but also η_a. A third definition of the "supply reduction factor" congruent with this approach is:

$$\bar{q}_s^a = \eta_a \cdot \bar{q}_s \tag{14}$$

At this point, the "actual performance ratio", PR^a, is defined, which gives the ratio of the actual structural supply to the seismic demand:

$$PR^a = \frac{F_e^{as}}{F_e^d} \tag{15}$$

Amongst others, actual to design strength ratios of materials, partial safety factors, conservative models for predicting member resistance, effects of structural elements not included in the analysis and effects of non-structural elements are responsible for η_a.

3. ON THE CALIBRATION OF THE REDUCTION FACTOR IN SEISMIC CODES

The ratio of F_e^s to F_d can be rewritten as the product of the performance ratio times the design reduction factor, if it is multiplied and divided by F_e^d:

$$\frac{F_e^s}{F_d} = PR \cdot q_d \tag{16}$$

This ratio can also be written as the product of q_s, the first definition of supply reduction factor, times the design structural overstrength, if it is multiplied and divided by F_{1y}:

$$\frac{F_e^s}{F_d} = q_s \cdot \eta_d \tag{17}$$

From equations (16) and (17):

$$PR = \eta_d \cdot \frac{q_s}{q_d} \tag{18}$$

The product of η_d times q_s is equal to $\bar{q}_s$, so equation (18) can be rewritten in the following form:

$$PR = \frac{\bar{q}_s}{q_d} \tag{19}$$

3.1. APPROACH 1

In order to calibrate the design reduction factor in the seismic code, q_d could be forced to tend to q_s. From equation (18), this first approach would imply forcing the performance ratio to be equal to the design structural overstrength.

$$if \quad q_d \to q_s \quad then \quad PR = \eta_d \tag{20}$$

The first approach together with the ULS verification of the seismic code, $\eta_d \geq 1$, assures a performance ratio equal to or greater than one, which is the performance objective of the ULS verification:

$$if \quad \left(q_d \to q_s \quad and \quad \eta_d \geq 1\right) \quad then \quad PR \geq 1 \tag{21}$$

3.2. APPROACH 2

Experience shows that the performance of well-designed structures can largely exceed the performance objective of the ULS of the seismic code. One of the sources of this good performance could be the design structural overstrength. If this is the case, it seems logical to include the design structural overstrength when calibrating the design reduction factor. $q_d \to \overline{q}_s$ could be forced in order to make the performance ratio equal to one, which is the optimal solution able to fulfil the performance objective of the ULS of the seismic code. From equation (19):

$$if \quad q_d \to \overline{q}_s \quad then \quad PR \to 1. \tag{22}$$

This second approach is senseless, since PR is insensitive to variations in q_d when $\eta_d > 1$. Including η_d in the calibration of q_d will not modify member proportioning, since a value of $\eta_d > 1$ indicates that ULS verification in the seismic code is irrelevant in member proportioning. Reduction of the seismic design load will not reduce the size of the structural element. Besides, from the safety of the ULS verification point of view, including η_d in the evaluation of q_d is clearly unsafe, since this amount is implicitly included in F_{1y} when the resistance of the structural member is compared with the internal design forces. Therefore, η_d cannot be included, for a second time, as a reduction of F_d . The second approach would be only justified if η_d were equal to one, when the resistance of the structural member that yields at first is controlled by the ULS verification of the seismic code. For this particular case, the second approach agrees with the first approach, resulting in the conclusion that the second approach makes sense only in the particular case in which it is equal to the first:

$$if \quad \eta_d = 1 \quad then \quad \overline{q}_s = q_s \tag{23}$$

In summary, including η_d in the evaluation of the design reduction produces an unsafe verification of the ULS under seismic loads, and it does not produce any economy in the structural design. A conservative lower bound of q_d can be obtained from analytical studies if it is calibrated in order to be equal to q_s :

$$q_d \to q_s \tag{24}$$

3.3. APPROACH 3

Post-earthquake investigations are of paramount importance in earthquake engineering. They are and will continue to be one of the main sources of information to support decisions in the calibration of seismic standards. However, it is necessary to estimate and exclude the design structural overstrength in the evaluation of q_d when calibrating the design seismic spectrum from the observation of building performance under past earthquakes. A higher bound from seriously damaged buildings could be obtained if q_d is calibrated in the following way:

$$q_d \to \frac{\overline{q}_s^a}{\eta_d} \tag{25}$$

The previous approach implicitly includes η_a in the calibration of q_d , and therefore the approach 3 includes the ratio of the actual to the assumed capacity by the code to resist an earthquake.

4. PARAMETRIC STUDY

The sample under study is shown in Table I. A total of 13,608 ductile frames have been studied. The number of storeys varies from 2 to 20. The number of bays varies from 2 to 5. The storey height is constant and is equal to 3.2 meters. The span length ranges from 5 to 9 meters. The design PGA varies from 1 to 4 meters per square second. The dead and live loads have been assumed to be equal to 4 and 2 kN per square meter. Three different steel grades have been considered, Fe360 and Fe430 for the beams and Fe430 and Fe510 for the columns. Three different soil classes according to Eurocode 8 have been considered. Two different inter-storey drift limits has been considered in the

verification of the SLS under seismic loads: 0.004 and 0.0075 defined as the inter-storey displacement divided by storey height. All the frames are designed to be ductile. The beam-to-column connections are rigid and full-strength.

Table I. Sample under study, which amounts to a total of 13,608 tested frames.

number of storeys	2 3 4 6 8 11 14 17 20
number of bays	2 3 5
storey height (m)	3.2
span length (m)	5. 7. 9.
design PGA (m/s2)	1 1.5 2. 2.5 3. 3.5 4.0
design drift limit	0.004 0.0075
dead load (kN/m2)	4.
live load (kN/m2)	2.
beam steel grades	Fe360 Fe430
column steel grades	Fe430 Fe510
soil class following Eurocode 8	A B C
beta Park-Ang parameter	0.15
earthquake duration	20.
Total number of frames under study	13608

5. DESIGN

All the structures have been designed according to Eurocode 3 and Eurocode 8. The flowchart in Figure 2 has been implemented in a computer program. The principle of Eurocode 8 that forces a mechanism where plastic hinges will form in the beams and in the base of the columns of the first storey is respected. To this aim, when proportioning the columns, the method based on the kinematic theorem of plasticity [14] is implemented in the design process. Furthermore, we verify that yielding of non-dissipative zones and member instability could not occur under the internal forces associated with the target plastic mechanism.

6. EVALUATION

6.1. Rotation capacity of steel members.

The rotation capacities of steel members will influence to a large extent the structural performance. The behaviour of a steel profile working in bending in the non-linear range and its influence in the local ductility supply depends on many parameters at material, cross section and member levels [15-16]. Experiments show a large scatter of local ductility supply with values of coefficient of variation which range from 0.4 to 0.9 depending on the slenderness ratio [17]. The variability of yield stress and strain hardening will have an important influence on the characteristic values of local ductility supply [18]. Strain hardening properties of the steel material from experimental and analytical evidence are likely to be one of the primary causes of the large variation of member ductility supply [17]. The softening branch in the moment-rotation curve in the post-critical range influences the rotation capacity [19].

Some methods use the kinematic theorem of plasticity to evaluate the rotation capacity of the steel member [15,20]. Other simplified methods compute the rotation from the integration of moment-curvature curve in the elastic and plastic range neglecting the rotation supplied in the post-buckling range [21-23]. These approaches can be interesting for structures under gravity loads, but they are too conservative in the case of seismic loads which are cyclic [15], where the structural system under horizontal load becomes very redundant.

Other simplified methods are based on formulas calibrated from test results [24-26], or from tests and numerical experiments using the FEM [27], and they account for the rotation capacity provided in the post-buckling range. The methods in [26] and [27] do not account for the influence of the axial force and thus cannot be used for beam-columns members.

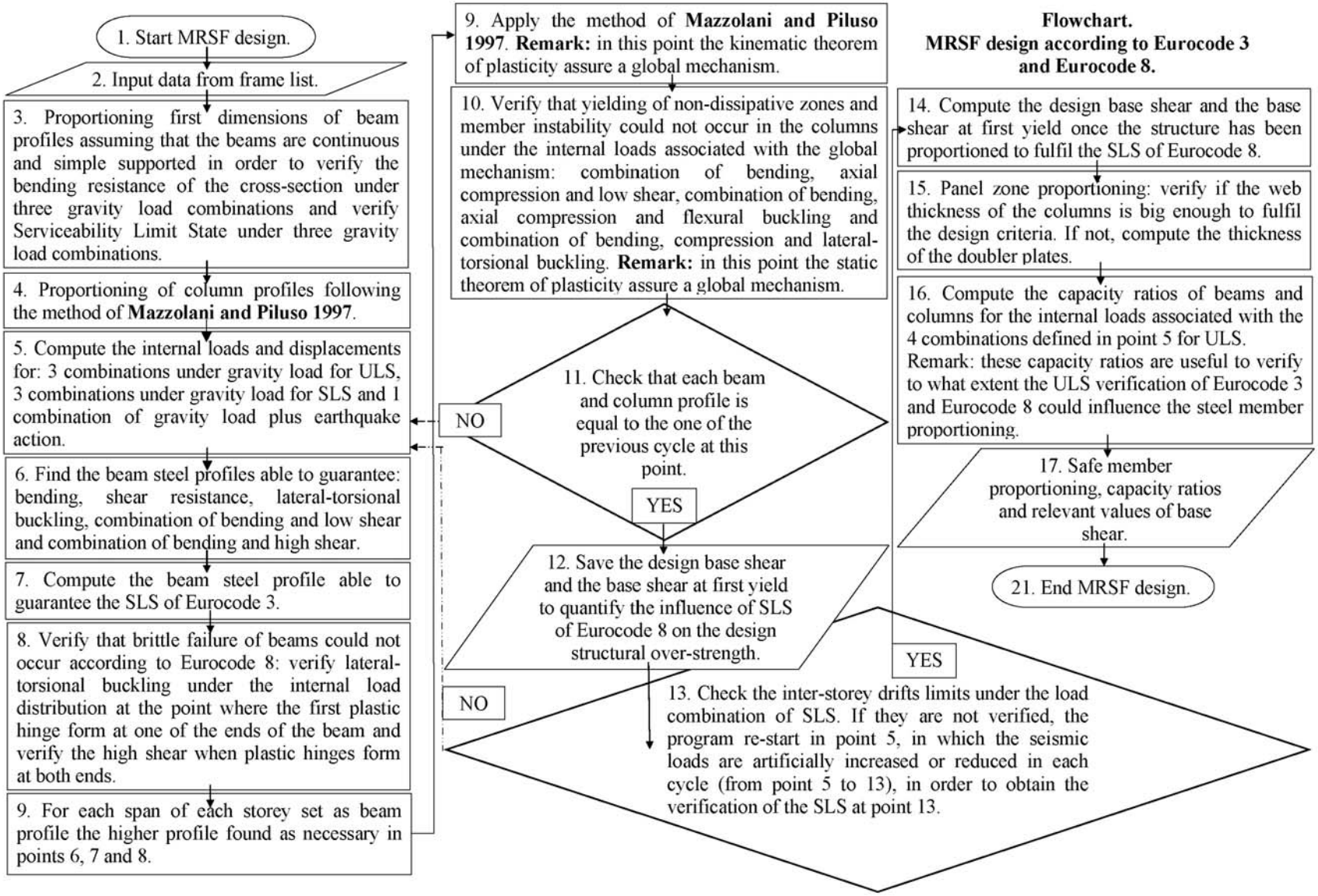

Figure 2. Design flowchart.

The empirical method [25] allows accounting for the most important parameters influencing the local ductility supply, and provides safe estimations if characteristics ratios of ultimate to yield steel strength are used. After some modifications and the validation of the method with experimental results, this method is used in the present study to estimate the ductility capacity of the steel members.

A modification has been applied to smooth the formulation [25] in order to avoid the discontinuity in the post-critical slope when the lateral torsional buckling increasing ratio is equal to the local buckling increasing ratio. The strain hardening ratio of the steel has been limited as proposed by [28]. A comparison of the modified formulation with 45 Standard Beam type 1 Tests (SB1T) performed in the literature [19,27,29-32] on steel profiles Class1 and 2 following Eurocode 3 provides a mean and COV of the ratios predicted to observed rotation capacity of 1.08 and 0.38 respectively; see Figure 3.

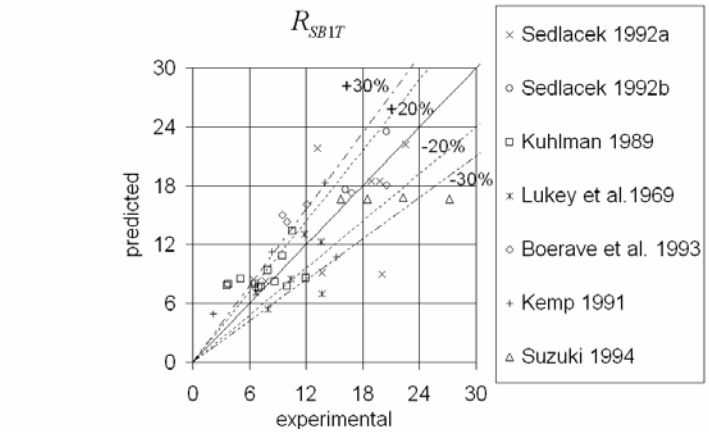

Figure 3. Experimental versus predicted rotation capacity ratios.

The mean and COV are very similar to those obtained in [16] using a plastic mechanism composed of plastic zones and yield lines. If we assume a normal distribution, a partial safety factor of $\gamma_\theta = 1.7$ will provide a predicted value lower than the expected value with a probability of 0.95. References [16] and [27] suggest a partial safety factor of $\gamma_\theta = 1.5$. We will use the value of $\gamma_\theta = 1.5$ proposed in the technical literature for design purposes in the present study.

The plastic moment will be the one defined in the Eurocodes. The increment of the capacity to dissipate energy due to moment overstrength will be accounted for with an equivalent increment of the local ductility supply.

6.2. Panel zone.

Panel zone can be the weakest element in the beam to column joint when the frame is submitted to lateral loads. Test results [33-38] show the possibility that the panel zone would yield in shear before the beams and columns reach their flexural capacities and demonstrate the importance of the panel zone on the behaviour of the beam to column joints, with important ductility supplies and hysteretic energy dissipations, which can reach values up to 50 % of the total hysteretic dissipated energy in the joint [39].

In order to accurately predict the response of a MRSF under horizontal loads, several simplified formulations have been proposed in the technical literature [37, 38, 40-41]. Although they agree on the elastic behaviour (elastic stiffness and yield forces), they differ on the non-linear representation.

A new formulation has recently been proposed [42] which improves the prediction for the cases where the flange of the columns are important, and takes into account the flexural deformation of the panel zone. In the present study, the quadrilateral model [37] implemented with the formulation [42] is used to model the panel zone. This choice allows representing the geometrical relation which exists between the distortion angle and the rotation, and the relative displacement at the frame members ends. Furthermore, it improves the shortcomings of [37] in the case of thick column flanges.

6.3. Cyclic behaviour of beam-to-column connections.

Brittle failures and poor ductile behaviour under cyclic loading in steel beam-to-column connections have been observed in the laboratory from 1960 up to now [43-55]. Systematically, a percentage of beam-to-column steel connections fail with undesirable brittle failure in each test programme, see for example [54, 55]. If we take a look at the database [56] formed of 513 tested steel-to-column joints, we can see that brittle failure always arises in a given percentage. These tests have been performed in a wide variety of connection types from the typical pre-Northridge beam-to-column connection to the wide pre-qualified connection details proposed in [57].

The present study aims to provide support for the design of new buildings. Theoretically, brittle failure of connections must be avoided in the design, but this premise will be difficult to implement in practice, and the connection performance will be highly dependent on its type, detailing, quality of welding and workmanship.

The β parameter of the damage model in [58] will be used in the present study to represent the sensitivity of the steel beam-to-column connection to low-cycle fatigue. In order to determine the range of interest, β has been evaluated on the basis of experimental tests [55] for the most usual beam-to-column connections used in Europe (beam welded to end-plate and bolted to the column). The ratio of the maximum plastic rotation demand, θ_p^d, to the plastic rotation supply, θ_p^s, quantifies the local damage index related to the maximum deformation. The ratio of the hysteretic energy, E_h, to the hysteretic energy under monotonic load, $M_y \cdot \theta_p^s$, quantifies the local damage index related to the energy dissipation, where M_y is the plastic moment. In order to make the local damage model, DM_θ, of Park and Ang congruent in the case of monotonic increasing load, $DM_\theta = 1$ at $\theta_p^d = \theta_p^s$, the local damage index will be:

$$DM_\theta = (1-\beta)\frac{\theta_p^d}{\theta_p^s} + \beta \cdot \frac{E_h}{M_y \cdot \theta_p^s} \tag{26}$$

In order to evaluate β from tests results:

$$\text{if} \quad DM_\theta = 1 \quad \text{then} \quad \beta = \frac{\theta_p^s - \theta_p^d}{E_h / M_y - \theta_p^d} \tag{27}$$

In the following, β will be treated as a parametric variable since it must depend on the connection details. But for this first parametric study, a default constant value of β seems to be sufficient for code calibration purposes. A conservative value of $\beta = 0.15$ is obtained from test results [55].

The reader must not be surprised by the high value of $\beta = 0.15$ since the value of β depends on the estimated values of local rotation supply, θ_p^s (see equation 27). The higher the value of θ_p^s, the higher the evaluated value of β. Since the method used to estimate θ_p^s is based on monotonically increasing static loads, θ_p^s is much higher than typical values assumed as acceptable in seismic codes for seismic cyclic loading, and therefore, the evaluation of β is much higher than usual values for steel structures. β is very sensitive to the assumed value of θ_p^s, but the computation of damage and the final result is not.

In order to illustrate the previous comment, we show the design plastic rotation supplies of the 8-storey MRSF designed according to Eurocode 3 and Eurocode 8 (see Tables II and III). Figure 1 represents the pushover analysis curve of this frame. The values of θ_p^s computed with the simplified method together with the application of the damage model with $\beta = 0.15$, both calibrated with experimental tests (see references [19,27,29-32] and [55]), produce a value of the maximum plastic rotation demands at the life-safety limit equal to 0.036 radians. Inter-storey drift demands in the range of 1.5 to 2 % of the storey height are reported from seriously damaged buildings. This corresponds to rotation demand up to 0.02 radians [59]. Although the values of θ_p^s for the beams provided by the simplified method (from 0.044 to 0.059 radians), largely exceed the assumed values of the maximum rotation supplies generally used in seismic codes (from 0.02 to 0.035 radians), the maximum rotation demands at the life-safety limit using $\beta = 0.15$ is 0.036 radians, which coincides well with maximum values accepted in seismic codes.

The simplified method is able to capture the influence of the steel profile depth on the plastic rotation supply. For a given span length, a higher depth of the steel profile is related to lower values

of plastic rotation supply.

The plastic rotation supplies of columns are influenced by the internal axial compression. They vary from 0.032 radians in the last storeys to 0.019 radians in the lower storeys. The plastic rotation supplies of columns are lower than the plastic rotation supplies of beams for three main reasons: 1) the internal axial compressions reduce the plastic rotation supplies, 2) the lower material increasing ratio of the higher steel grade of the columns produces a concentration of plasticity, and 3) the shorter lengths of the columns increase the moment gradient producing a concentration of plasticity which also reduces the plastic rotations supplies.

The total number of plastic hinges formed at the life safety limit is 70, $DM = 0.8$. The global mechanism has not been entirely developed. There are not plastic hinges in the columns of the first storey, showing that the frame is able to dissipate large amounts of energy, and to reach important values of ductility supplies before the global mechanism is entirely formed.

Table II. 8-storey MRSF. Design plastic rotation supply, θ_p^s, and plastic rotation demand, θ_p^d, at life-safety limit –units in radians-.

		Number of beam span				
Storey		1	2	3	4	5
08	θ_p^s	.054	.059	.059	.059	.054
	θ_p^d	.000 .000	.000 .000	.000 .000	.000 .000	.000 .000
07	θ_p^s	.053	.059	.059	.059	.053
	θ_p^d	.007 .005	.006 .006	.006 .006	.006 .006	.005 .008
06	θ_p^s	.053	.058	.058	.058	.053
	θ_p^d	.021 .020	.020 .020	021 .020	.020 .020	.020 .022
05	θ_p^s	.048	.053	.053	.053	.048
	θ_p^d	.031 .030	.030 .030	.031 .031	.030 .030	.030 .032
04	θ_p^s	.048	.048	.048	.048	.048
	θ_p^d	.036 .035	.035 .035	.035 .035	.035 .035	.035 .036
03	θ_p^s	.044	.048	.048	.048	.044
	θ_p^d	.033 .032	.032 .032	.032 .032	.032 .032	.032 .033
02	θ_p^s	.044	.048	.048	.048	.044
	θ_p^d	.023 .021	.022 .022	.022 .022	.022 .022	.021 .023
01	θ_p^s	.044	.047	.047	.047	.044
	θ_p^d	.008 .007	.007 .007	.008 .008	.007 .007	.007 .009

Table III. 8-storey MRSF. Design plastic rotation supply of columns. - θ_p^s in radians-.

	Column vertical axis					
Storey	1	2	3	4	5	6
08	.032	.031	.031	.031	.031	.032
07	.026	.025	.025	.025	.025	.026
06	.023	.023	.023	.023	.023	.023
05	.023	.024	.026	.026	.024	.023
04	.022	.024	.024	.024	.024	.022
03	.023	.023	.023	.023	.023	.023
02	.021	.021	.021	.021	.021	.021
01	.019	.020	.019	.019	.020	.019

6.4. Evaluation flow chart.

A flowchart summing up the procedure to evaluate the structural capacity, based on the N2 method [4], is presented in Figure 4. The plastic mechanism, the rotation supply of the steel members and the β parameter influence the ductility capacity and the endurance capacity to low-cycle fatigue of the

structural system. The spectral intensity and the dimensionless parameter γ [60], which relates the hysteretic dissipated energy per unit mass to the maximum relative displacement, determine the capacity of the seismic action to produce damage.

The influence of the soil class is accounted for in the low-cycle fatigue effect, since the soil class influences the value of γ. Stiffer soils are richer in higher frequencies, and thus the number of equivalent cycles and the influence of the low-cycle fatigue on the structural damage will be higher. Each frame has been designed for a given soil class (which influences the elastic and design spectrums). In the evaluation the structural capacity, we remain congruent with the soil class used in the design in the computation of γ. For comprehensive information on γ parameter, which control the low fatigue effect, please see reference [60].

The global damage index is computed as the weighted average of the local damage indexes. The weights are assumed to be proportional to the dissipated energy accordingly to the N2 method.

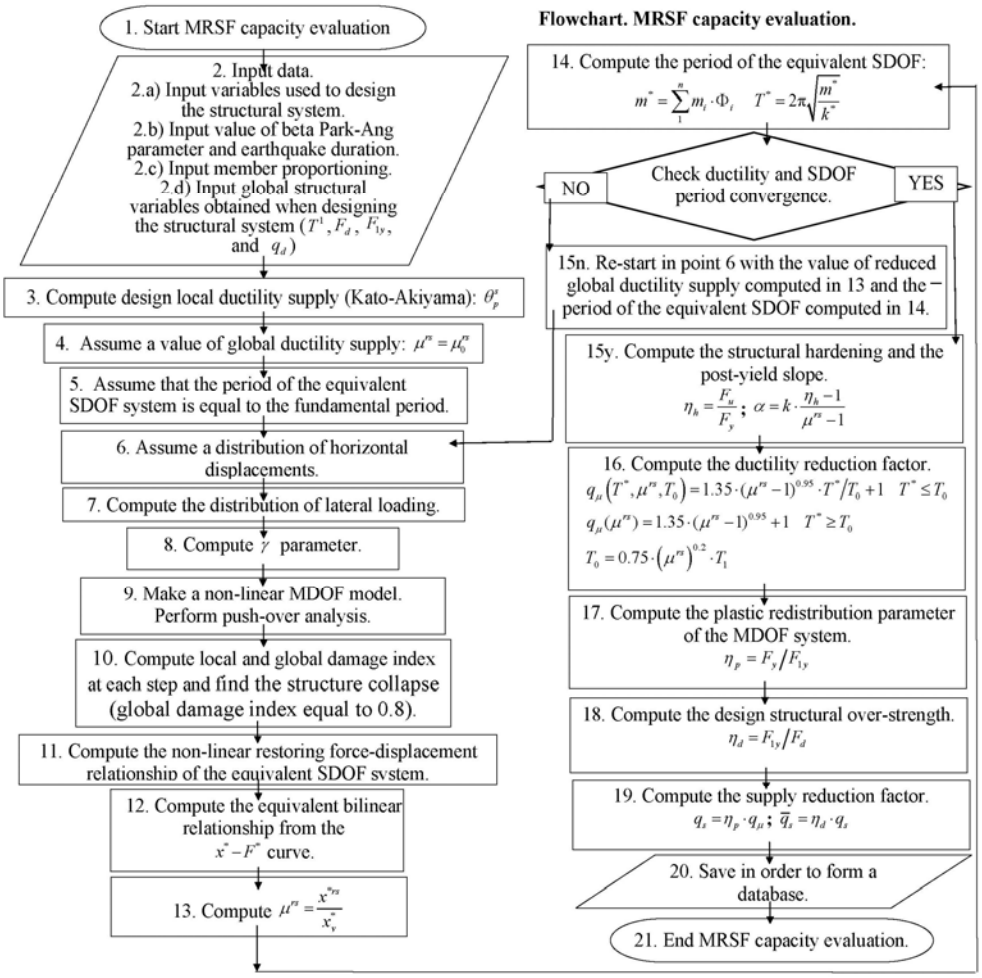

Figure 4. Evaluation flowchart.

7. RESULTS OF THE PARAMETRIC STUDY

Hereafter, the results of the parametric study are reported (see reference [61] for more detailed information). In the following figures, each point represents the numerical result for one frame under study. The lines of the graphs are trend lines from the numerical results at the same design PGA.

7.1. Design structural overstrength, η_d.

The values of η_d range from 1.4 to 16.6 (see Figure 5), showing that the resistances of the

structural elements are systematically higher than the resistance necessary to fulfil the proportioning of dissipative zones in the ULS verification of Eurocode 8. η_d is very sensitive to the design PGA, the inter-storey drift limits at high values of design PGA, the soil class and the structural period. η_d is quite sensitive to the steel grade of the beams. It moderately depends on the inter-storey drift limits at low values of design PGA, on the number of bays and on the span length. It is insensitive to the steel grade of the columns.

Low values of η_d are related to: 1) high values of design PGA, 2) high values of the inter-storey drift limit, 3) low values of steel grade of the beams, 4) soil class with high amplification of ground PGA, 5) increasing number of storeys, 6) increasing number of bays, 7) long span length at high values of design PGA, and 8) short span length at low values of design PGA.

At low values of design PGA, gravity loads and capacity design criteria control the member proportioning. At high values of design PGA, Serviceability Limit requirements of Eurocode 8 and capacity design criteria control the member proportioning.

The design is never controlled by the proportioning of dissipative zones in the Ultimate Limit State verification of Eurocode 8. Depending on the situation, this is partially due to the structural type itself, which is very flexible.

7.2. Plastic redistribution of internal forces and structural hardening, $\eta_p \cdot \eta_h$.

The plastic redistribution of internal forces times the structural hardening, $\eta_p \cdot \eta_h$, ranges from 1.02 to 2.8 (see Figure 6). Therefore, the limiting value of 1.6 in Eurocode 8 can be largely exceeded. The parametric study shows a correlation between η_d and $\eta_p \cdot \eta_h$: higher values of η_d are generally related to higher values of $\eta_p \cdot \eta_h$. This correlation increases the dispersion in the performance ratio. $\eta_p \cdot \eta_h$ is very sensitive to the design PGA, the soil class and the inter-storey drift limit. It is also quite sensitive to the steel grade of the beams and columns. A clear correlation of $\eta_p \cdot \eta_h$ with the number of bays and the span length cannot be observed. The values proposed in Eurocode 8 (1.2 if plastic analysis is not performed and an upper bound of 1.6 if plastic analysis is performed) seem to be appropriate for high seismic regions. This values will be largely exceeded for lower values of design PGA, a_d. This confirms that the code background is mostly based on structures designed for high seismic regions.

7.3. Reduced ductility supply, μ^{rs}.

The values of μ^{rs} vary from 1.6 to 4.6 (see Figure 7). The value of 5 assumed in Eurocode 8 for ductile MRSF is higher than the values resulting from this parametric study.

μ^{rs} is the most stable global structural parameter. It is not sensitive or poorly sensitive to the design PGA (in the case of frames with long span lengths), the number of bays, the inter-storey drift limits, the steel grade of beams and the steel grade of columns (when the number of storeys is high). μ^{rs} is moderately sensitive to the span length, the design PGA for long span frames and the soil class. μ^{rs} is quite sensitive to the period of the structure and the steel grade of columns in the case of frames with a low number of storeys.

7.4. Supply reduction factor, q_s.

The dispersion in q_s is enormous: the values range from 1.9 to 12.46 and the limits assumed in Eurocode 8 range from 6 to 8 (see Figure 8). The significant dispersion in the results confirms the dispersion found in the literature and suggests that a constant value cannot be provided for design purposes. For structural periods that range from 0.4 to 1.5 seconds, and for design values of PGA higher than 0.3 g, the ULS value proposed in Eurocode 8 is much higher than the values resulting from the parametric study.

As stated in 3.3, it is pertinent to recall than the values of ductility supply and reduction factor in seismic codes are mostly based on and will continue to be mostly based on the observation of building performance under past earthquakes. The ductility supply and reduction factor proposed in seismic codes account not only for the ductility supply, but they implicitly account for the structural overstrength. Therefore, it is not surprising that the ductility supply and reduction factor proposed in

Eurocode 8 could be higher than the values of ductility of supply and reduction factor obtained in the parametric study.

q_s is sensitive to the period of the structure, the design PGA, the span length, the inter-storey drift limit, the steel grade of beams, the steel grade of columns and the soil class. If we take into account the large number of input variables that influence its value, the significant dispersion of q_s is not surprising. A clear correlation between the supply reduction factor and the number of bays cannot be observed.

7.5. Performance ratio, PR.

The performance ratio for all designed structures is higher than one. This means that the equivalent elastic supply spectrum is higher than the elastic spectrum of Eurocode 8. This is true for the 13,608 frames under study. PR varies from 1.2 to 14.3 (see Figure 9). The performance objective of the ULS verification is reached for the 13,608 frames under study, but in many cases this is due to code restraints that have nothing to do with the proportioning of the dissipative zones in ULS verification of Eurocode 8. It is clear from the dispersion that a uniform damage design procedure can only be based on guidance for conceptual design. Calibration of the code will not produce structures with uniform values of PR.

The performance ratio is very sensitive to the design PGA, the inter-storey drift limit for high values of design PGA and the soil class. Although in the parametric study there are lots of interdependent and coupled variables, the main reasons are probably the followings:

1. The higher the value of PGA the lower the value of η_d and thus, the lower the value of PR.
2. For high values of design PGA, the lower the inter-storey drift limit, the higher the stiffness of the structural elements, the higher the resistance, and therefore, the higher the value of η_d and PR.
3. The stiffer the soil, the higher the number of equivalent imparted cycles and the higher the amplification. This reduces η_d, increases the number of equivalent imparted cycles, increase the low fatigue effect and reduce the ductility supply. The reduction of η_d and the ductility supply reduces PR.

The performance ratio is moderately sensitive to the number of bays, the span length, the inter-storey drift limit for low values of design PGA, the steel grade of the beams and the steel grade of the columns.

8. CONCLUSIONS

The following conclusions apply to ductile MRSF designed according Eurocode 3 and Eurocode 8:

1. The seismic structural supply is much higher than the seismic demand for each of the 13,608 MRSF under study. The present parametric study indicate that the application of Eurocode 3 and Eurocode 8 produce structures with values of Performance Ratio always higher than 1.2. This means that in the worse case the seismic capacity is at least 20 % higher than required.
2. The performance ratio can be rewritten as the product of the design structural overstrength times the ratio between supply and design reduction factor:

$$PR = \eta_d \cdot \frac{q_s}{q_d} \tag{28}$$

The first term, η_d, ranges from 1.4 to 16.6 while the second term, q_s/q_d, ranges from 0.3 to 2. Many structures can survive and earthquake thanks to the design structural overstrength resulting from the application of Eurocode 3 and Eurocode 8.

3. We can roughly say, that the seismic capacity due to structural overstrength, $\eta_d \cdot \eta_p \cdot \eta_h$, is in general higher than the seismic capacity due to ductility supply.
4. The structural performance and the cost of a MRSF poorly depend on the “design reduction factor”, q_d. Reduction of the cost could only be reached with a good conceptual design. The combination of guidance for conceptual design and calibration of the seismic code could provide safety and optimisation.
5. The most stable and least scattered global structural parameter was the global ductility supply: this

could allow a more reliable definition of the reduction of the spectrum, which would only be controlled by the "ductility reduction factor". Besides, estimation of the ultimate capacity under horizontal load of a MRSF using plastic analysis is very simple and is not time consuming.

6. From the authors' consideration, the best solution for the design of MRSF is perform rigid-plastic analysis to determine the ultimate capacity of a MRSF and reduce the elastic spectrum to the design spectrum with the "ductility reduction factor", which is much more stable than the supply reduction factor. This solution will also solve the necessity of evaluating the actual internal forces in the non-dissipative zones from plastic analysis.

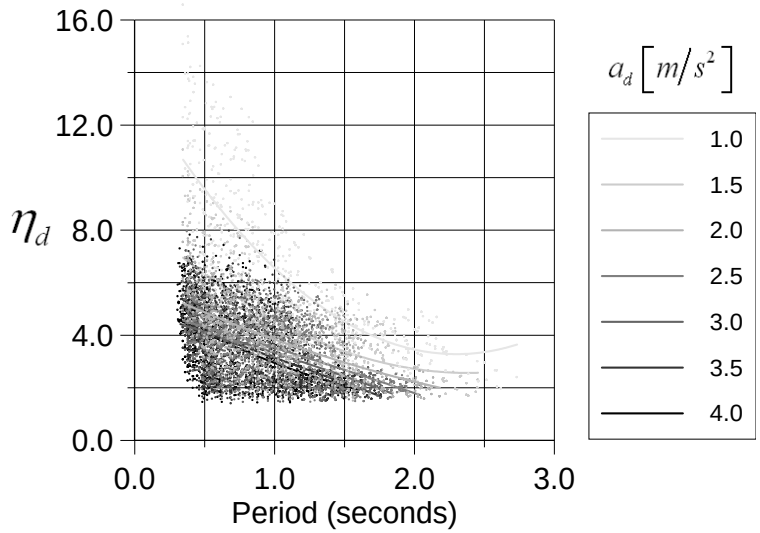

Figure 5. Design structural overstrength: influence of design PGA.

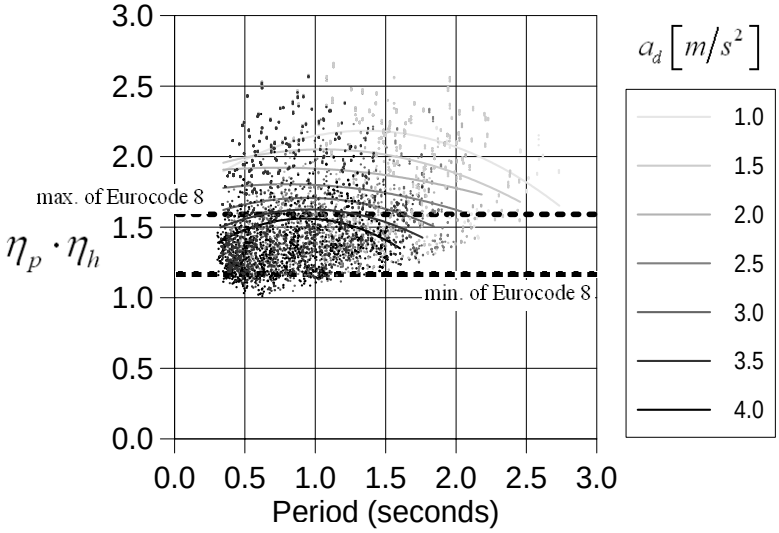

Figure 6. Influence of design PGA on $\eta_p \cdot \eta_h$ ($\eta_p \cdot \eta_h$ is close to the plastic redistribution parameter, α_u/α_1, defined in Eurocode 8).

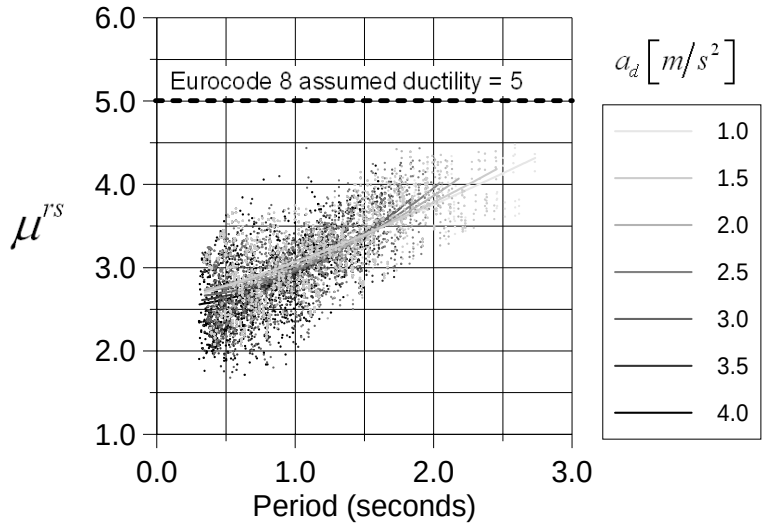

Figure 7. Reduced global ductility supply: influence of design PGA.

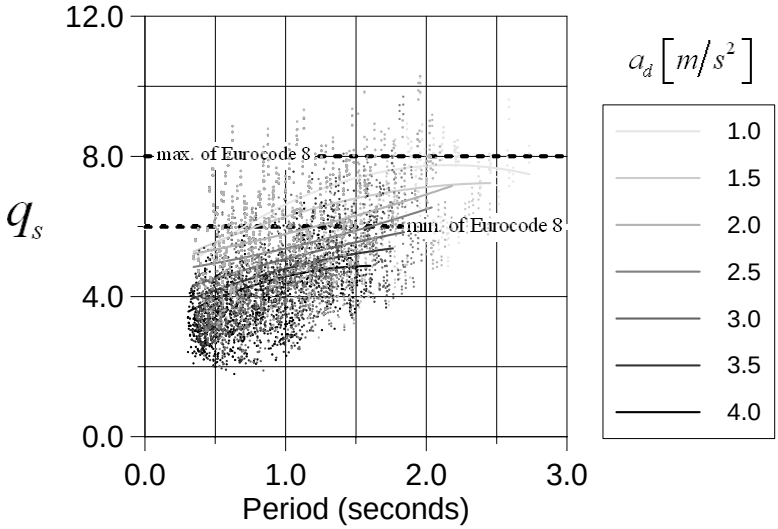

Figure 8. Supply reduction factor: influence of design PGA.

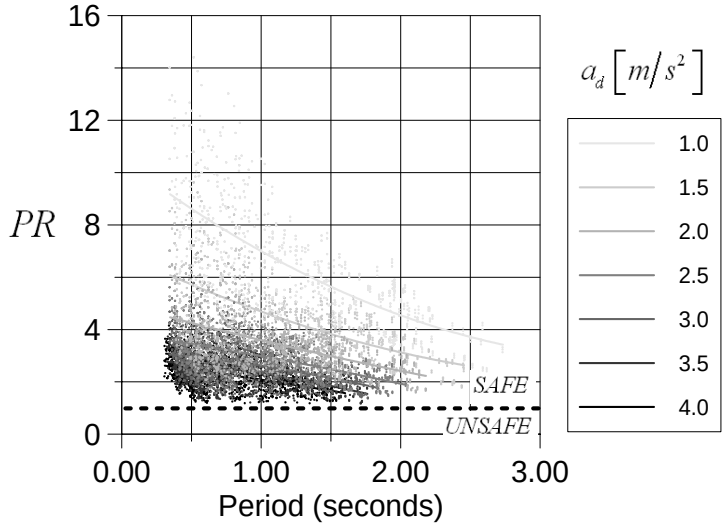

Figure 9. Performance ratio: influence of design PGA.

REFERENCES

1. Krawinkler H. Challenges and progress in performance based earthquake engineering. *International Seminar on Seismic Engineering for Tomorrow – In Honor of Professor Hiroshi Akiyama*, Tokyo, Japan, 1999.
2. Fajfar, Peter. Capacity spectrum method based on inelastic demand spectra. *Earthquake Engineering & Structural Dynamics* 1999, **28**(9):979-993.
3. Design of structures for earthquake resistance. CEN Eurocode 8. 2002.
4. Fajfar P, Gaspersic P. The N2 method for the seismic damage analysis of RC buildings. *Earthquake Engineering & Structural Dynamics* 1996, **25**(1):31-46.
5. Design of steel structures. CEN Eurocode 3. 1992.
6. Newmark NM, Hall JF. Earthquake spectra and design. Earthquake Engineering Research Institute. Berkeley, California, 1982.
7. Nassar AA, Krawinkler H. Seismic demands for SDOF and MDOF systems. BLUME-095, John A. Blume Earthquake Engineering Centre, Stanford, California, 1991.
8. Miranda E, Bertero VV. Evaluation of strength reduction factors for earthquake-resistant design. *Earthquake Spectra* 1994, **10**(2):357-379.
9. Vidic T, Fajfar P, Fischinger M. Consistent inelastic design spectra: strength and displacement. *Earthquake Engineering & Structural Dynamics* 1994, **23**(5):507-521.
10. ECCS Manual on Design of Steel Structures in Seismic Zones. European Convention for Construction Steel Work. 1988.
11. Structural response modification factors. Applied Technology Council (**A**TC-19). 1995.
12. An investigation of the correlation between earthquake ground motion and building performance. Applied Technology Council (ATC-10). 1982.
13. A critical review of current approaches to earthquake-resistant design. Applied Technology Council (ATC-34). 1995.
14. Mazzolani FM, Piluso V. Plastic design of seismic resistant steel frames. *Earthquake Engineering & Structural Dynamics* 1997, **26**(2):167-191.
15. Gioncu V, Petcu D. Available rotation capacity of wide-flange beams and beam-columns, Part 1: Theoretical approaches. *Journal of Constructional Steel Research* 1997, **43**(1-3):161-217.
16. Gioncu V, Petcu D. Available rotation capacity of wide-flange beams and beam-columns, Part 2: Experimental and numerical tests. *Journal of Constructional Steel Research* 1997, **43**(1-3):219-244.
17. Nakashima M. Uncertainties associated with ductility performance of steel building structures. *Seismic Design Methodologies for the Next Generation of Codes*, A.A. Balkema, Rotterdam and Brookfield, Vermont, Bled, Slovenia, 1997, 111-118.
18. Chryssanthopoulos MK, Manzocchi GME, Elnashai AS. Probabilistic assessment of ductility for earthquake resistant design of steel members. *Journal of Constructional Steel Research* 1999, **52**(1):47-68.
19. Kuhlmann U. Definition of flange slenderness limits on the basis of rotation capacity values. *Journal of Constructional Steel Research* 1989, **14**:21-40.
20. Climenhaga JJ, Johnson RP. Moment-rotation curves for locally buckling beam. *Journal of the Structural Division*, ASCE, 1972, **98**(ST6):1239-1254.
21. Kemp AR. Interaction of plastic local and lateral buckling. *Journal of Structural Engineering* 1985, **111**(10):2181-2196.
22. Kato B. Rotation capacity of H-section members as determined by local buckling. *Journal of Constructional Steel Research* 1989, **13**(2-3):95-109.
23. Mazzolani FM, Piluso V. Evaluation of the Rotation Capacity of Steel Beams and Beam-Columns. 1st Cost C1 Workshop, Strasbourg 1992, 28-30.
24. Mitani I, Makino M. Post local buckling behavior and plastic rotation capacity of steel beam-columns. *Seventh World Conference o Earthquake Engineering*, Istanbul 1980, Vol. **6**:493-500.
25. Kato B, Akiyama H. Analysis on inelastic flexural torsional buckling of H-shaped steel beams columns. *Trans. of A.I.J.* 1978, No. 264.
26. Nakamura T. Strength and deformability of H-shaped steel beams and lateral bracing requirements. *Journal of Constructional Steel Research* 1988, **9**(3):217-228.
27. Spangemacher R, Sedlacek G. Zum Nachweis ausreichender Rotations-fähigkeit von Fli-essgelenken bei der Anwendung des Fliessgelenkver-fahrens. *Stahlbau* 1992, **61**(H 11):329-339.
28. Lay MG, Galambos TV. Inelastic beams under moment gradient. *Journal of the Structural Division*, ASCE, 1967, **93**(ST1):381-399.
29. Lukey AF, Adams PF. Rotation capacity of beams under moment gradient. *Journal of the Structural Division*, ASCE 1969, **95**(ST6):1173-1188.
30. Kemp AR, Dekker NW. Available rotation capacity in steel and composite beams. *The Structural Engineer*, 1991, **69**(5), 88-96.

31. Boeraeve P, Lognard B, Janss J, Gerardy JC, Schleich JB. Elasto-plastic behaviour of steel frameworks. *Journal of Constructional Steel Research* 1993, **27**:3-21
32. Suzuki T, Ogawa T, Ikarashi K. A study on local buckling behaviour of hybrid beams. *Thin-Walled Structures* 1994, **19**:337-351
33. Naka et al. Research on the behavior of steel beam-to-column connections in the seismic-resistant structure. *Fourth World Conference on Earthquake Engineering*, Santiago, Chile 1969, Vol. II, pages B3-1 to B3-14.
34. Bertero VV. 1969. Seismic behavior of steel beam-to-column connection subassemblages. Proceedings of the Fourth World Conference on Earthquake Engineering, Chilean Association on Seismology and Earthquake Engineering, Santiago, Chile, Vol. II, 1969, pages B3-31 to B3-44
35. Bertero VV, Popov EP, Krawinkler H. 1972. Beam-Column Subassemblages Under Repeated Loading. Journal of the Structural Division, ASCE, 98, ST5, May 1972, pages 1137-1159
36. Becker ER. Panel zone effect on the strength and stiffness of rigid steel frames. Research report, Mechanical Lab., University of Southern California; 1971.
37. Krawinkler H, Bertero VV, Popov EP.1975. Shear behavior of steel frame joints. Journal of the Structural Division, ASCE, 101, ST11, Nov 1975, pages 2317-2336, Proc. Paper 11717
38. Lu, Wang, Lee. Cyclic behavior of steel and composite joints with panel zone deformation. Proceedings of the Ninth World Conference on Earthquake Engineering, Japan, Tokyo 1989, Vol. IV, pages 701-706.
39. Sotirov P, Rangelov N, Ganchev O, Georgiev T, Milev J, Petkov Z. Chapter 3: Cyclic behaviour of beam-to-column bare steel connections, 3.3 Influence of haunching. *Moment Resistant Connections of Steel Frames in Seismic Areas: Design and Reliability*, E & FN Spon, London; New York, 2000, pages 245-265
40. Fielding DJ, Chen WF. Steel frame analysis and connection shear deformation. *Journal of the Structural Division*, ASCE 1973, **99**(ST1):1-18.
41. Tsai KC, Popov EP. Steel beam-column joints in seismic moment resisting frames. UCB/EERC-88/19, Berkeley: Earthquake Engineering Research Center, University of California, 1988.
42. Kim KD, Engelhardt MD. Monotonic and cyclic loading models for panel zones in steel moment frames. *Journal of Constructional Steel Research* 2002, **58**(5-8):605-635.
43. Popov EP, Pinkney RB. Reliability of steel beam-to-column connections under cyclic loading. *Proceedings of the Fourth World Conference on Earthquake Engineering*, Chile, Santiago 1969, Vol. II, pages B3-15 to B3-30.
44. Popov EP, Bertero VV. Cyclic loading of steel beams and connections. *Journal of the Structural Division*, ASCE 1973, **99**(ST6):1189-1204.
45. Popov EP, Amin NR, Louie JC, Stephen RM. Cyclic behavior of large beam-column assemblies. *Earthquake Spectra* 1985, **1**(2):203-238.
46. Popov EP and Tsai KC. Performance of Large Seismic Steel Moment Connections Under Cyclic Loads. SEAONC. 56th annual Convention 1987.
47. Popov EP, Tsai KC and Engelhardt MD. On Seismic Steel Joints and Connections. SEAONC. 57th Annual Convention 1988.
48. Anderson JC and Linderman RR. 1991. Post earthquake repair of welded moment connections. CE 91-04, Dept. of Civil Engineering, Univ. of Southern California, Los Angeles 1991, Vol 1.
49. Engelhardt MD, Husain AS. Cyclic-loading performance of welded flange-bolted web connections. *Journal of Structural Engineering* 1993, **119**(12):3537-3550.
50. Engelhardt MD, Sabol TA. Testing of welded steel moment connections in response to the Northridge earthquake. American Institute of Steel Construction, 1994.
51. Yang TS, Popov EP. Experimental and Analytical Studies of Steel Connections and Energy Dissipators, Report UCB/EERC-95/13, Earthquake Engineering Research Center, California, Berkeley 1995.
52. Shuey BD, Engelhardt MD, Sabol TA. Testing of repair concepts for damaged steel moment connections, Report to the SAC Joint Venture, Ferguson Structural Engineering Laboratory, The University of Texas, Austin, TX, 1996.
53. Uang CM, Bondad D. Static cycle testing of pre-Northridge and haunch repaired steel moment connections, Report no. SSRP-96/02. Division of Structural Engineering, University of California. San Diego, CA, 1996.
54. Engelhardt MD, Sabol TA. Reinforcing of steel moment connections with cover plates: benefits and limitations. *Engineering Structures* 1998, **20**(4-6):510-520.
55. Beg D, Plumier A, Remec C, Sanchez-Ricart L. Influence of strain rate. In: Mazzolani FM, editor. Moment resistant connections of steel frames in seismic areas-design and reliability. London: E & FN Spon; 2000, p. 167–216 [chapter 3.1].
56. Connection test database. SAC Steel Project. http://www.sacsteel.org/connections/data.xls
57. FEMA-350. Recommended Seismic Design Criteria for New Steel Moment-Frame Buildings, 2000.
58. Park YJ, Ang AH. 1985. Mechanistic seismic damage model for reinforced concrete. *Journal of Structural Engineering* 1985, **111**(4):722-739.
59. Plumier A. General report on local ductility. *Journal of Constructional Steel Research* 2000, **55**:91-107.
60. Fajfar P, Vidic T. Consistent inelastic design spectra: hysteretic and input energy. *Earthquake Engineering & Structural Dynamics* 1994, **23**(5):523-537.

61. Sanchez-Ricart, L. Seismic Performance of Ductile Moment Resisting Steel Frames. First Step for Eurocode 8 Calibration. Ph.D. Thesis. University of Liege, 2004.